

## Deformed nature of the $6^-$ states in $^{26}\text{Al}$ observed by the $(\alpha, t)$ reaction

M. Yasue, H. Sato, and T. Hasegawa\*

*Institute for Nuclear Study, University of Tokyo, Tanashi, Tokyo 188, Japan*

J. Takamatsu, T. Terakawa, and T. Nakagawa

*Department of Physics, Tohoku University, Sendai 980, Japan*

K. Hatori

*Japan Atomic Industrial Forum, Incorporated, Minato-ku Tokyo 105, Japan*

R. J. Peterson

*Nuclear Physics Laboratory, University of Colorado, Boulder, Colorado 80309*

(Received 18 January 1989)

The  $^{25}\text{Mg}(\alpha, t)^{26}\text{Al}$  reaction has been studied at  $E_\alpha = 50$  MeV in the region of excitation energy from 5 to 10 MeV with an energy resolution of 20 keV. The fragmentation of the strengths for the stretched  $6^-$  states is found to be consistent with the calculation for an oblatelly deformed nucleus, in contrast to the prolate shape of the ground-state band.

### I. INTRODUCTION

A large fragmentation of the spectroscopic strengths for the stretched  $6^-$  states in  $A=26$  nuclei with a configuration of  $(0d_{5/2})^{-1}(0f_{7/2})$  has been found through various reaction processes<sup>1</sup> such as inelastic electron scattering and stripping reactions,  $(\alpha, t)$ ,<sup>2</sup>  $(\alpha, ^3\text{He})$ ,<sup>3</sup>  $(^3\text{He}, d)$ ,<sup>4</sup>  $(d, n)$ ,<sup>5</sup> and  $(\alpha, d)$ .<sup>6</sup>

Previously, Zamick<sup>7</sup> pointed out the possibility of two modes of excitation of the stretched states, the shell-model-like particle-hole excitation and the collective rotator mode. On the basis of the Nilsson model, Peterson *et al.*<sup>4</sup> deduced a deformed nature of the  $6^-$  states in  $^{26}\text{Mg}$  and  $^{26}\text{Al}$  nuclei with a negative deformation, and pointed out that the fragmentation of the  $6^-$  strengths in  $^{26}\text{Mg}$  and  $^{26}\text{Al}$  is due to the deformed structure of these nuclei.

In the calculation,<sup>4</sup> the stripping strength ratio of the first  $6^-$  state to the second  $6^-$  state should be 2.1 for  $\beta = -0.3$ . The ratio obtained from the  $^{25}\text{Mg}(\alpha, t)^{26}\text{Al}$  data<sup>4</sup> at  $E_h = 55.2$  MeV is 1.2 for  $6^-; T=0$  states. The ratio is 1.1 in the  $(\alpha, t)$  reaction at  $E_\alpha = 81$  MeV.<sup>2</sup> These results show a large deviation from the calculation.

The high-resolution study<sup>8</sup> of  $^{26}\text{Al}$  by Endt *et al.* via the  $(p, \gamma)$  reaction revealed that the 7.540-MeV  $2^-; 1$  and the 7.458-MeV  $5^-; 0$  states also lie close to the second  $6^-; 0$  state at  $E_x = 7.529$  MeV. The previous work<sup>4</sup> on the  $(^3\text{He}, d)$  reaction with an energy resolution of 38 keV was insufficient to deduce cross sections for the second  $6_2^-; 0$  state due to the adjacent peaks. Thus further spectroscopic study on  $^{26}\text{Al}$  with a better energy resolution is required to test the applicability of the Nilsson model to the fragmentation of the  $6^-$  strength in  $A=26$  nuclei.

In the present work, the  $^{25}\text{Mg}(\alpha, t)^{26}\text{Al}$  reaction is studied with better energy resolution around the excitation energy from 5 to 10 MeV, and the deduced spectro-

scopic strengths for the  $6^-$  states are compared to the prediction<sup>4</sup> from the Nilsson model. In order to check the reliability of the distorted-wave Born approximation (DWBA) analyses, the spectroscopic strengths for the  $5^-$  and  $4^-$  states are also compared with the previous work<sup>2</sup> on the  $(\alpha, t)$  reaction at the higher incident energy of 81 MeV.

### II. EXPERIMENTAL PROCEDURE

The experiment was performed with a momentum-analyzed 50-MeV  $\alpha$ -particle beam from the Institute for Nuclear Studies (INS) sector-focusing cyclotron. Reaction products were analyzed by the quadrupole-dipole-dipole magnetic spectrometer<sup>9</sup> with a setting of  $\Delta\Omega = 1$  msr and  $\Delta\theta = \pm 0.33^\circ$ . Details of the experimental procedure are described elsewhere.<sup>10</sup>

An 80- $\mu\text{g}/\text{cm}^2$  and 97.9% enriched target of self-supporting  $^{25}\text{Mg}$  foil was prepared by a rolling method, and the thickness was checked by comparing the yields for elastic scattering with those from a  $^{25}\text{Mg}$  foil for which the thickness was calibrated to be 0.45  $\text{mg}/\text{cm}^2$  from the weight. Figure 1 shows a typical momentum spectrum for the  $^{25}\text{Mg}(\alpha, t)^{26}\text{Al}$  reaction at  $\theta_{\text{lab}} = 20^\circ$ . The energy resolution of the spectrum is 20 keV full width at half maximum, nearly twice as good as seen in Ref. 4 and five times better than seen in Ref. 2.

The peaks around the 7.529-MeV  $6^-; 0$  state are composed of three peaks with centroid energies cited from the  $(p, \gamma)$  work,<sup>8</sup> as shown in Fig. 2, where the spectrum is analyzed by a peak fitting program.<sup>11</sup> The energy scale is calibrated by the prominent peaks at  $E_x = 5.685, 6.084,$  and  $9.267$  MeV and by the contaminant peaks due to  $^{12}\text{C}$  and  $^{16}\text{O}$ .

Obtained cross sections are shown in Figs. 3–5. Absolute errors in the cross sections are estimated to be no more than 10%.

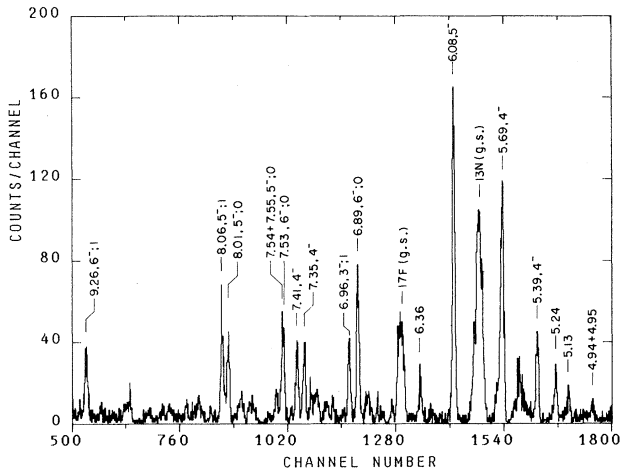


FIG. 1. A typical momentum spectrum for the  $^{25}\text{Mg}(\alpha, t)^{26}\text{Al}$  reaction at  $E_\alpha = 50$  MeV and  $\theta_{\text{lab}} = 20^\circ$ .

### III. DWBA ANALYSES

The zero-range (ZR) DWBA calculations are more dependent on the incident energy and on potential parameters than the exact-finite-range (EFR) DWBA calculations. The zero-range approximation tends to overestimate the contributions from the nuclear interior. The local-energy approximation<sup>12</sup> in the ZR calculation can correct the overestimation, but the corrections are still insufficient to obtain consistent spectroscopy over the wide range of the incident energy, and independently from the types of reaction channels such as  $(\alpha, t)$  and  $(^3\text{He}, d)$ , etc. The EFR description is more reliable over the wide range of momentum transfer. At the present, however, the resonance form factor for unbound states is available only for the ZR description using the program DWUCK4.<sup>13</sup> Therefore, an additional correction on the normalization of the ZR calculation was used in our pre-

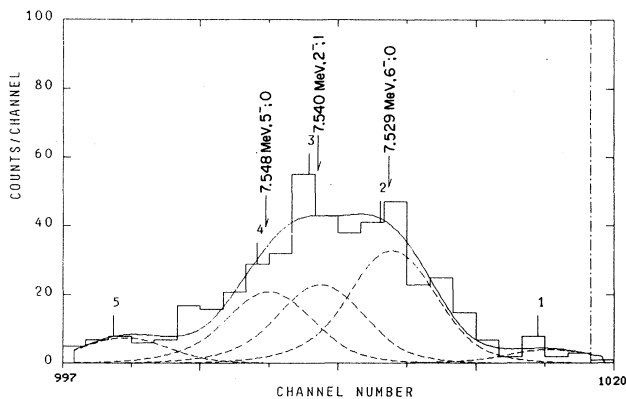


FIG. 2. Peaks around  $E_x = 7.54$  MeV in Fig. 1 are fitted by three peaks (dotted curves) with centroid energies as indicated in the figure and with a peak shape the same as the neighboring peaks at  $E_x = 8$  and 6.89 MeV. A solid curve is the envelope of the dotted curves.

vious works<sup>2,4</sup> by comparing the cross sections calculated by ZR and EFR approximations.

In order to deduce reliable spectroscopic information from the ZR DWBA analyses of the  $^{25}\text{Mg}(\alpha, t)^{26}\text{Al}$  reaction, a normalization constant for the ZR DWBA calculation is set to give the same cross-section values as the EFR DWBA analyses for the bound  $4^-$  state at  $E_x = 5.69$  MeV.

In the EFR DWBA code "TWOFRN",<sup>14</sup> cross sections are expressed

$$\frac{d\sigma}{d\Omega_{\text{expt}}} = C^2 S \frac{d\sigma}{d\Omega_{\text{calc}}} \quad (1)$$

In a case of the  $^{25}\text{Mg}(\alpha, t)^{26}\text{Al}$  reaction, the isospin Clebsch-Gordan factors  $C^2$  are  $\frac{1}{2}$  for both  $T_f = 0$  and 1, and the light particle spectroscopic factor  $s = 2$ . The spectroscopic factor  $S$  should be unity for the stripping to an empty single-particle state. In the EFR DWBA calculation with the TWOFRN code,<sup>14</sup> the  $p$ - $t$  relative wave function  $\phi$  in an  $\alpha$  particle is approximated to be of the Hulthen type. An analytic form for  $\phi U$  is further approximated to be a Yukawa-type interaction of  $V_0 \exp(-\xi r)/r$ , where  $V_0 = 133.26$  MeV and  $\xi = 1.33 f_m^{-1}$ .

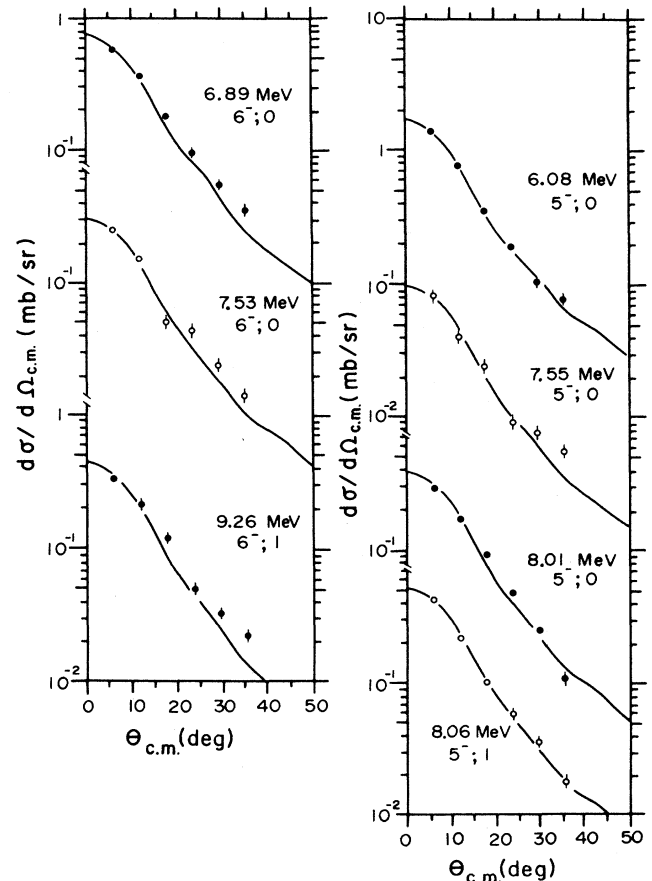


FIG. 3. Angular distributions for the  $^{25}\text{Mg}(\alpha, t)^{26}\text{Al}$  reaction leading to the  $6^-$  and  $5^-$  states. Solid curves are ZR DWBA calculations for the  $0f_{7/2}$  transfer with DWUCK4.

$U$  is an effective potential between a proton and a triton. The interaction parameters<sup>15</sup> are set to reproduce the rms radius of the  $\alpha$  and the separation energy of a proton from an  $\alpha$ . The form factor for the bound proton is generated by the usual separation energy method in a Woods-Saxon potential.

The potential parameters used in the present analyses are listed in Table I, where the parameter for the  $\alpha$  channel is obtained to reproduce the elastic scattering data, as shown in Fig. 6, by searching with the program SEARCH.<sup>16</sup>

IN the ZR DWBA code "DWUCK4,"<sup>13</sup> cross sections are expressed as

$$\frac{d\sigma}{d\Omega_{\text{expt}}} = D_0^2 C^2 S \frac{2J_f + 1}{(2j + 1)(2J_i + 1)} \frac{d\sigma}{d\Omega_{\text{DW4}}} . \quad (2)$$

By comparing cross sections calculated by Eqs. (1) and (2) for the  $0f_{7/2}$  single-particle transfer to the 5.69-MeV  $4^-$  state, the  $D_0^2$  value in Eq. (2) is set to

$$D_0^2 = 6.8 \times 10^4 \text{ MeV}^2 \text{ fm}^3 , \quad (3)$$

where the local-energy approximation is used to approximate finite range effects in the ZR calculation, using a range parameter of 0.67 fm.

The  $D_0^2$  value in Eq. (3) is a little smaller than the generally accepted value of  $7.1 \times 10^4 \text{ MeV}^2 \text{ fm}^3$  for the  $(\alpha, t)$  reaction.<sup>15-19</sup>

The form factor for the bound state in the ZR calculation is the same as in the EFR calculation. For the unbound state above  $E_x = 6.3 \text{ MeV}$ , a resonance form factor is used in the ZR DWBA calculation.<sup>13</sup>

#### IV. RESULTS AND DISCUSSION

Figure 3 shows the cross sections for the  $6^-$  and  $5^-$  states observed in the present work. Curves, which are normalized to the data at forward angles, are ZR DWBA calculations for the  $0f_{7/2}$  single-particle transfer. As listed in Table II, deduced spectroscopic factors for the  $6^-$  and  $5^-$  states show good consistency with the previous works on  $(\alpha, t)$  (Ref. 2) and  $(^3\text{He}, d)$  (Ref. 4) reactions except for the second  $6^-; T=0$  state at  $E_x = 7.529 \text{ MeV}$ .

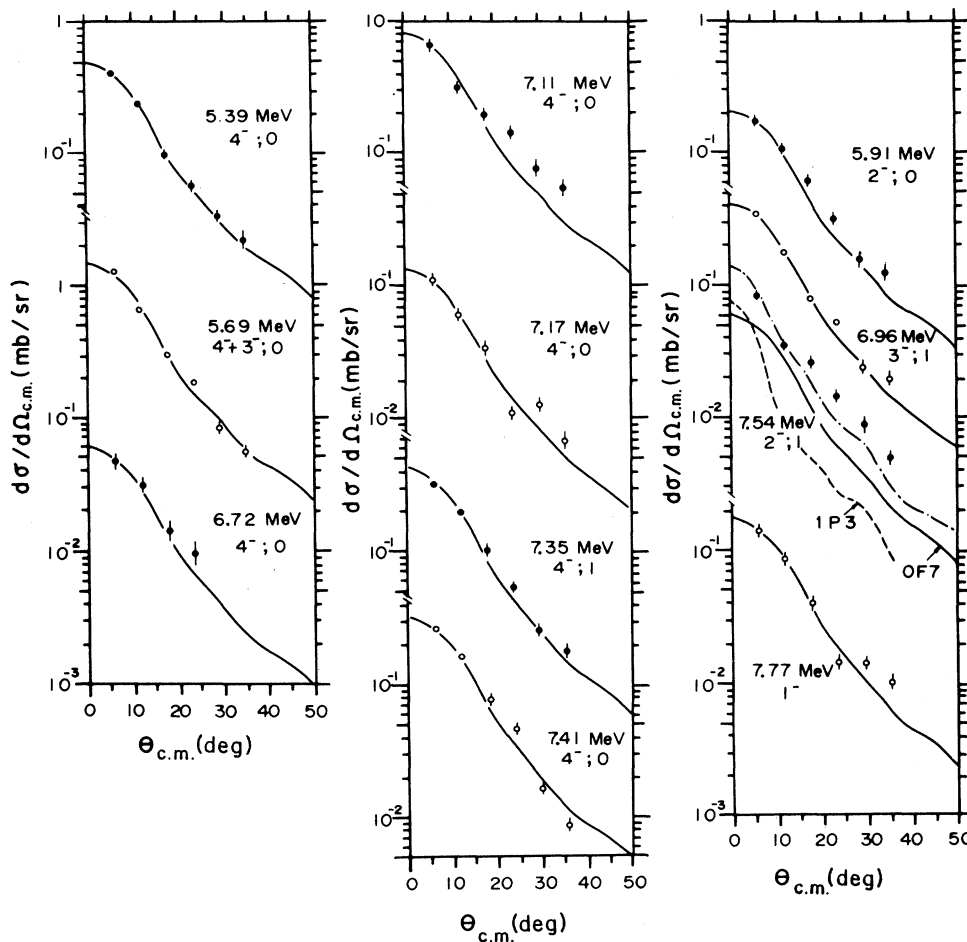


FIG. 4. Angular distributions for the  $4^-$ ,  $3^-$ ,  $2^-$ , and  $1^-$  states in  $^{26}\text{Al}$  observed in the present work. Solid curves are ZR DWBA calculations for the  $0f_{7/2}$  transfer. Dashed and dashed-dotted curves for the 7.52-MeV  $2^-; 1$  state indicate a  $1p_{3/2}$  transfer and a fit by the  $0f_{7/2}$  and  $1p_{3/2}$  curves, respectively.

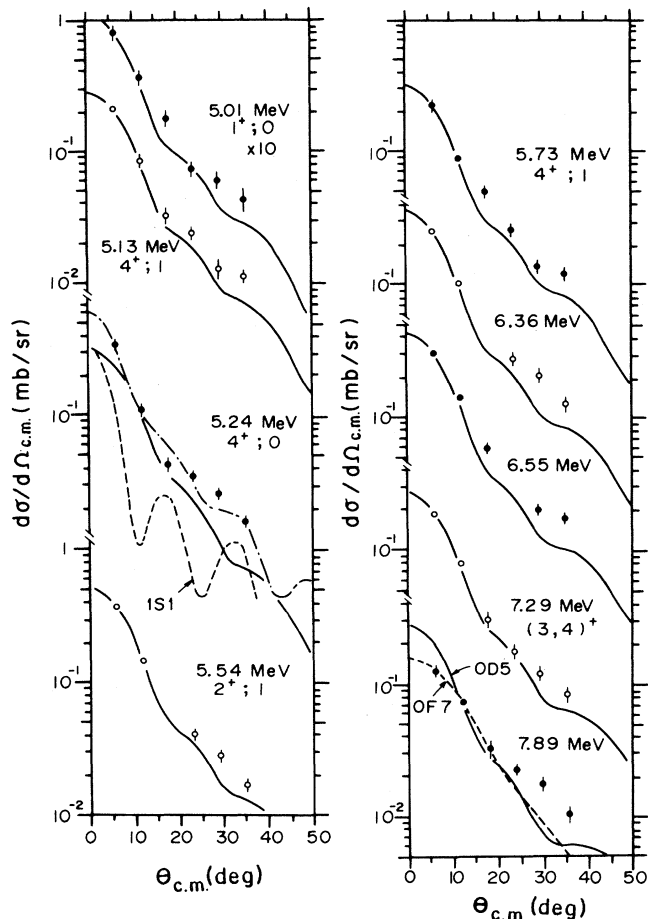


FIG. 5. Angular distributions for the positive-parity states in  $^{26}\text{Al}$ . Solid curves are ZR DWBA calculations for  $0d_{5/2}$  transfer. Dashed and dashed-dotted curves for the 5.24-MeV  $3^+$  state indicate a  $1s_{1/2}$  transfer and a fit by the  $0d_{5/2}$  and  $1s_{1/2}$  curves, respectively. Data for the 5.01-MeV state have been multiplied by a factor of 10.

As seen in Fig. 2, the spectrum around the  $6^-$  state can be reproduced by the three peaks found in the  $(p, \gamma)$  work.<sup>8</sup> However, in the previous works<sup>2,4</sup> on the  $(\alpha, t)$  and  $(^3\text{He}, d)$  reactions, the triplet was analyzed as a single peak of the  $6^-$  state. Thus the present result on the 7.53-MeV  $6^-$  state presents a smaller spectroscopic

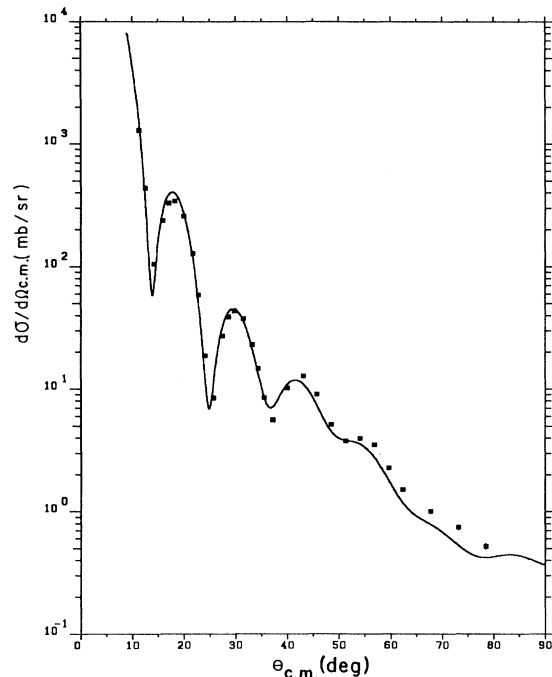


FIG. 6. Angular distribution for elastic scattering of 50-MeV  $\alpha$  particles from  $^{25}\text{Mg}$  and the fit obtained with the optical model using the parameters listed in Table I.

strength than the previous works.

The 6.083-MeV state was assigned in the  $(\alpha, d)$  reaction to be the first  $5^-; 0$  state.<sup>6</sup> The large spectroscopic factor for the  $5^-$  state compared to those for the  $6^-$  states indicates the simple  $0f_{7/2}$  particle  $0d_{5/2}$  hole structure of the state. The fact is also confirmed by the small spectroscopic strength of the second  $5^-; 0$  state at  $E_x = 7.548$  MeV. The relatively large strength for the third  $5^-; 0$  state of 8.011 MeV is interpreted in the  $(\alpha, d)$  work<sup>6</sup> to be caused by a mixture of  $0f_{7/2}$  and  $0f_{5/2}$  components. An isospin mixture<sup>8</sup> of the 8.011-MeV state with the adjacent  $5^-; 1$  state at  $E_x = 8.067$  MeV can also increase the single-particle strength of the  $5^-; 0$  state. Such a mixture is pointed out by Endt *et al.*<sup>8</sup>

Compared to the  $5^-; 0$  states, the smaller strength for the first  $6^-; 0$  state and the larger fragmentation of the

TABLE I. Potential parameters (Standard Wood-Saxon type) used in the DWBA analyses of the  $^{25}\text{Mg}(\alpha, t)^{26}\text{Al}$  reaction.  $JR/A1A2$  means a volume integral of the real part of the potential per nucleon.

Channel	$V_R$ (MeV)	$r_R$ (fm)	$a_R$ (fm)	$W_V$ (MeV)	$r_W$ (fm)	$a_W$ (fm)	$V_{1s}$ (MeV)	$r_c$ (fm)	$JR/A1A2$ (MeV fm <sup>3</sup> )
$\alpha + ^{25}\text{Mg}^a$	184.3	1.16	0.752	27.5	1.37	0.751	0	1.3	451
$t + ^{26}\text{Al}^b$	110.4	1.14	0.805	20.4	1.49	0.903	0	1.4	356
Bound state <sup>c</sup>		1.25	0.65				6	1.25	

<sup>a</sup>Searched to reproduce the elastic scattering data at  $E_\alpha = 50$  MeV.

<sup>b</sup>Cited from Ref. 17.

<sup>c</sup>For unbound states above  $E_x = 6.3$  MeV, a resonance form factor is used (Ref. 13). These parameters have been used for all analyses of  $A = 26$  in the present series (Refs. 2–4).

TABLE II. Spectroscopic information for  $0f_{7/2}$  stripping to high spin states in  $^{26}\text{Al}$  studied by the  $^{25}\text{Mg}(\alpha, t)^{26}\text{Al}$  reaction at  $E_\alpha = 50$  MeV. Error in excitation energy is  $\pm 5$  keV.

Previous work <sup>a</sup>		Present work			Spectroscopic factors		
$E_x$ (MeV)	$J^\pi; T$	$E_x$ (MeV)	$NL2J$	$\sigma_{\text{int}}$ (mb)	Present work ( $\alpha, t$ )	Previous works ( $^3\text{He}, d$ ) <sup>b</sup>	( $\alpha, t$ ) <sup>c</sup>
6.892	$6^-; 0$	6.892	$0F7$	0.16	0.17	0.13	0.16
7.529	$6^-; 0$	7.527	$0F7$	0.06	0.09	0.11	0.15
9.264 <sup>c</sup>	$6^-; 1$	9.267	$0F7$	0.10	0.22	0.17	0.20
6.083	$5^-; 0^d$	6.084	$0F7$	0.33	0.38	0.31	0.32
7.548	$5^-; 0$	7.550	$0F7$	0.02	0.03		
8.011	$5^-; 0$	8.008	$0F7$	0.08	0.15	0.10	0.14
8.067	$5^-; 1$	8.065	$0F7$	0.10	0.20	0.18	0.19
5.394	$4^-; 0$	5.394	$0F7$	0.10	0.20	0.10	0.10
5.676	$4^-; 0$	5.676	$0F7$	0.21	0.26	0.31 <sup>e</sup>	0.35 <sup>e</sup>
5.692	$3^-; 0$	5.692	$0F7$	0.08	0.12		
6.724	$4^-; 0$	6.726	$0F7$	0.01	0.02		
7.109	$4^-; 0$	7.107	$0F7$	0.02	0.03		
7.168	$4^-; 0$	7.163	$0F7$	0.03	0.04		
7.348	$4^-; 1+(0)$	7.350	$0F7$	0.09	0.16		
7.410	$4^-; 0^d+(1)$	7.413	$0F7$	0.07	0.12		

<sup>a</sup>( $p, \gamma$ ) in Ref. 8 and ( $d, \alpha$ ) in Ref. 18.

<sup>b</sup>( $^3\text{He}, d$ ) at 55 MeV in Ref. 4.

<sup>c</sup>( $\alpha, t$ ) at 81 MeV in Ref. 2.

<sup>d</sup>Isospin assignment from ( $\alpha, d$ ) at 64.7 MeV in Ref. 6.

<sup>e</sup>The doublet at 5.676 and 5.692 MeV is not separated. These values are given by assuming the doublet to be a  $4^-$  state.  $\sigma_{\text{int}}$  means integrated cross section over the range of angles shown in Figs. 3–5:  $\sigma_{\text{int}} = 2\pi \int d\sigma/d\Omega \sin\theta d\theta$ .

$6^-; 0$  states are confirmed in the present work. Such a fragmentation may be ascribed to the unbound nature of the  $6^-$  states. The first  $5^-; 0$  state is bound by 0.2 MeV. The unbound  $0f_{7/2}$  particle can become effectively bound by a core if the core has a mixture of excited  $0\hbar\omega$  particle-hole components. In the Nilsson-scheme diagram, such an excited core is described as deformed. In the case of the  $6^-$  states in  $^{26}\text{Al}$ , the lowest  $6^-; 0$  or 1 state has the largest spectroscopic strength among the  $6^-$  states of  $T=0$  or 1. Namely, the core is negatively deformed in the picture of the Nilsson diagram.

Peterson *et al.*<sup>4</sup> described the fragmentation of the strength for the  $6^-$  states in  $^{26}\text{Al}$  with a deformation of  $\beta = -0.3$ . As states in Sec. III, the deformation leads to the strength ratio of  $S(6_1^-)/S(6_2^-) = 2.1$ . The present result shows the ratio to be 1.9, consistent with the picture. It is to be noted that the deformation is different in sign from that for the positive-parity states of the ground-state band of  $^{26}\text{Al}$ .<sup>20</sup>

Cross sections for the other negative-parity states are shown in Fig. 4, and their spectroscopic information is in Tables II and III. Shapes of the angular distributions for the  $4^-$  states are well described by the angular momentum transfer  $L=3$  only. In the ( $d, n$ ) reaction at  $E_d = 25$  MeV,<sup>5</sup> components of  $L=1$  and 3 transfers are needed to reproduce the shape of the angular distribution for the 6.724-MeV  $4^-$  state, because the ( $d, n$ ) reaction is matched to lower angular momentum transfer than the present ( $\alpha, t$ ) reaction. The ( $\alpha, t$ ) reaction at  $E_\alpha = 50$  MeV and  $E_x = 5$ –10 MeV emphasizes angular momen-

tum transfer  $L=4$  or 5.

The assignment of  $4^-$  states is cited from previous works by Endt *et al.*<sup>8,18</sup> They showed that the 7.35- and 7.41-MeV states have isospin-mixed structure. The ( $\alpha, d$ ) cross sections for the latter are 1.7 times larger than those for the former.<sup>6</sup> Namely, the 7.35-MeV state has a 37%  $T=0$  component. The larger ( $\alpha, d$ ) cross section for the 7.41-MeV  $4^-$  state may be caused by the mixture of a  $0d_{3/2}$  component to the  $(0d_{5/2})^{-1}(0f_{7/2,5/2})$  configurations for the  $4^-$  state, as discussed in our previous work.<sup>6</sup>

In Fig. 4, cross sections for the 5.69-MeV state are sums of those for the second  $4^-; 0$  state at  $E_x = 5.676$  MeV and the 5.692-MeV  $3^-; 0$  state. In Table II, spectroscopic strengths for the two states are listed explicitly. The second  $4^-$  state has a larger strength than the first  $4^-$  state at  $E_x = 5.394$  MeV, indicating a complicated structure of the first  $4^-$  state. The 5.692-MeV  $3^-$  state is the third  $3^-; 0$  state.<sup>18</sup> In the spectrum of Fig. 1, other low-lying  $3^-; 0$  states<sup>18</sup> at  $E_x = 5.457$  and 5.598 MeV are negligibly small. Different from the case of the  $T=0$ ,  $4^-$ , and  $3^-$  states, the first  $T=1$ ,  $4^-$ , and  $3^-$  states have spectroscopic strengths comparable to those for the second  $4^-; 0$ , state and for the third  $3^-; 0$  state, respectively. The low-lying  $T=0$ ,  $4^-$ , and  $3^-$  states with small spectroscopic strengths may be generated by a core-polarization effect.<sup>21</sup>

Results for the positive-parity states are shown in Fig. 5 and in Table III. The assignment of their spin-parity is also cited from Refs. 8 and 18. Present results are con-

TABLE III. Spectroscopic information for low-spin states in  $^{26}\text{Al}$  studied by the  $^{25}\text{Mg}(\alpha, t)^{26}\text{Al}$  reaction at  $E_\alpha = 50$  MeV.

Previous work <sup>a</sup>		Present work		$\sigma_{\text{int}}$ (mb)	Spectroscopic factors
$E_x$ (MeV)	$J^\pi; T$	$E_x$ (MeV)	$NL2J$		
5.916	$2^-; 0$	5.918	$0F7$	0.05	0.10
6.964	$3^-; 1$	6.965	$0F7$	0.08	0.18
7.540	$2^-; 1$	7.541	$0F7; 1P3$	0.02	0.06, 0.42
7.773	$1^-; 0$	7.772	$0F7$	0.04	0.24
5.010	$1^+; 0$	5.010	$0D5$	0.02	0.14
5.131	$4^+; 1$	5.129	$0D5$	0.04	1.12
5.245	$4^+; 0$	5.246	$0D5; 1S1$	0.06	0.19, 0.96
5.545	$2^+; 1$	5.545	$0D5$	0.08	0.46
5.726	$4^+; 1$	5.727	$0D5$	0.05	0.17
6.362		6.364	$0D5$	0.06	$2.12/(2J_F + 1)$
6.555		6.551	$0D5$	0.07	$2.75/(2J_F + 1)$
7.291	$(3, 4)^+$	7.294	$0D5$	0.04	$2.39/(2J_F + 1)$
7.891	$4^+; 1$	7.890	$(0D5)$ or $(0F7)$	0.04	0.37 or 0.07

<sup>a</sup>Cited from Refs. 8 and 18.

sistent with their assignment except for the 7.891-MeV state. The shape of the angular distribution for the state is reproduced better by the  $L=3$  transfer than by the  $L=2$  transfer, leaving a possibility of the state having a negative parity.

## V. CONCLUSION

Present work on the  $^{25}\text{Mg}(\alpha, t)^{26}\text{Al}$  reaction leading to the negative-parity states has shown that the deduced spectroscopic strengths for the  $0f_{7/2}$  transfer are in good consistency with the previous works on the  $(\alpha, t)$  reaction<sup>2</sup> at  $E_\alpha = 81$  MeV and on the  $(^3\text{He}, d)$  reaction<sup>4</sup> at  $E_h = 55.2$  MeV, except for the important second  $6^-; 0$  level, for which we now provide a more reliable result with better resolution. In our present and previous analyses,<sup>2,4</sup> the zero-range DWBA calculation is normalized to give the same cross-section values for a bound state with a simple structure as does the exact finite range DWBA calculation. This procedure provides reliable spectroscopic strengths for the bound and unbound states over

the wide range of momentum transfer.

For the  $4^-$  and  $3^-$  states of  $^{26}\text{Al}$ , the strength distribution for  $T=0$  states reflects complex core-coupled configurations compared to those for the  $T=1$  states. For the  $0f_{7/2}$  stripping strength to the  $5^-$  states, more concentration into the lowest  $T=0$  and 1 states is found than is the case for the  $6^-$ ,  $4^-$ , and  $3^-$  states.

The smaller concentration of the  $0f_{7/2}$  strength for the stretched  $6^-$  states than that for the  $5^-$  states may be ascribed to the unbound nature of the  $6^-$  states. Fragmentation of the strength between the first and second  $6^-; 0$  states is consistent with the previous analyses<sup>4</sup> for a negative deformation of  $\beta = -0.3$ . The deformation is different in sign from that for the positive-parity ground-state band.

## ACKNOWLEDGMENTS

The authors are obliged to Dr. Sugai for the preparation of the thin  $^{25}\text{Mg}$  target. Numerical calculations were carried out with the M780 INS central computer.

\*Present address: Faculty of Engineering, Miyazaki University, Miyazaki 889-21, Japan

<sup>1</sup>M. A. Plum, Ph.D. thesis, University of Massachusetts, 1985 (unpublished).

<sup>2</sup>R. J. Peterson *et al.*, Phys. Rev. C **33**, 31 (1986).

<sup>3</sup>J. J. Kraushaar *et al.*, Phys. Rev. C **34**, 1530 (1986).

<sup>4</sup>R. J. Peterson *et al.*, Phys. Rev. C **38**, 1130 (1988).

<sup>5</sup>J. Takamatsu, Masters thesis, Tohoku University (unpublished).

<sup>6</sup>M. Yasue *et al.* (unpublished).

<sup>7</sup>L. Zamick, Phys. Rev. C **29**, 667 (1984).

<sup>8</sup>P. M. Endt, P. Dewit, and C. Alderliesten, Nucl. Phys. **A459**, 61 (1986).

<sup>9</sup>S. Kato, M. H. Tanaka, and T. Hasegawa, Nucl. Instrum. Methods **154**, 19 (1978).

<sup>10</sup>M. Yasue, T. Tanabe, S. Kubono, J. Kokame, M. Sugitani, Y. Kadota, Y. Taniguchi, and M. Igarashi, Nucl. Phys. **A391**, 377 (1982).

<sup>11</sup>M. Yasue and T. Wada, Institute for Nuclear Studies Report No. 670, 1988 (unpublished).

<sup>12</sup>P. J. A. Buttle and L. J. B. Goldfarb, Proc. Phys. Soc. **83**, 701 (1964); Gy. Bencze and J. Zimany, Phys. Lett. **9**, 246 (1964); F. G. Perey and D. S. Saxon, *ibid.* **10**, 107 (1964).

<sup>13</sup>DWUCK4, a zero-range DWBA code written by P. D. Kunz, University of Colorado.

<sup>14</sup>TWOFNR, an exact-finite-range DWBA code written by M. Igarashi (unpublished).

<sup>15</sup>M. Igarashi, Phys. Lett. **78B**, 379 (1978).

<sup>16</sup>T. Wada, Institute of Physical and Chemical Research Rep. **46**, 21 (1970).

- <sup>17</sup>R. W. Barnard *et al.*, Nucl. Phys. **A108**, 641 (1968).  
<sup>18</sup>D. O. Boerma, A. R. Arends, P. M. Endt, W. Gruebler, V. Konig, P. A. Schmelzbach, and R. Risler, Nucl. Phys. **A449**, 187 (1986).  
<sup>19</sup>J. R. Shepard, W. R. Zimmerman, and J. J. Kraushaar, Nucl. Phys. **A275**, 189 (1977).  
<sup>20</sup>N. Takahashi *et al.*, Phys. Rev. C **23**, 1305 (1981).  
<sup>21</sup>A. Arima and H. Horie, Progr. Theor. Phys. **12**, 623 (1954).